

Supporting Information for the article “Single-Molecule Fluorescence Imaging of Interfacial DNA Hybridization Kinetics at Selective Capture Surfaces”

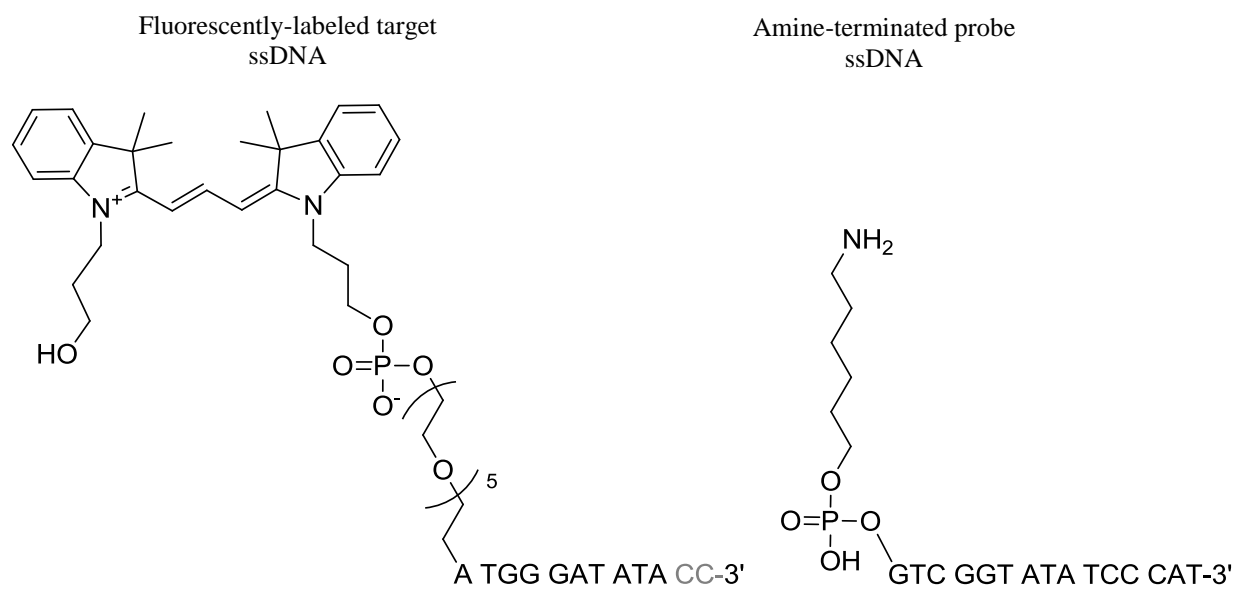
Eric M. Peterson and Michael W. Manhart, and Joel M. Harris *

Department of Chemistry
University of Utah
315 South 1400 East
Salt Lake City, UT 84112-0850

Contents:	Chemical and Material Sources	Page S-2
	Chemical Structures of Target, Control, and Probe DNA	Page S-3
	Oligonucleotide Immobilization onto Glass Surfaces	Page S-4
	Image Analysis for Detecting and Counting Molecules	Page S-5
	Measuring Γ_{\max} with 12-mer target ssDNA.....	Page S-10
	Fluorescence Background Correction with Scrambled Cy3-ssDNA.....	Page S-16
	Measuring Single-Molecule Residence Times	Page S-17
	Influence of Photobleaching on Measured Dissociation Rates	Page S-18
	High-speed Imaging to Detect Adsorbed target ssDNA	Page S-20
	Fluorescence Hybridization Measurements in Free-Solution.....	Page S-22
	Derivation of Equilibrium Fluorescence Expressions in Equation 5.....	Page S-24
	Description of Video Files.....	Page S-25
	References.....	Page S-26

Chemicals and Material Sources. All water used was purified to a resistivity of 18.2 M Ω ·cm using a Thermo Scientific GenPure UV water system. Single-stranded DNA (ssDNA) was synthesized and HPLC purified by the University of Utah HSC Core facility, and the sequences are detailed in the main text. Target DNA concentrations in solutions were determined by using a GE NanoVue Plus UV-Vis spectrometer to measure absorbance of the Cy3 fluorophore at 548 nm, with a molar absorptivity of 136,000 M⁻¹ cm⁻¹ (from manufacturer, <http://www.glenresearch.com/Technical/Extinctions.html>). Gold Seal glass 22x22 mm no. 1.5 coverslips, sodium bicarbonate (Macron, 100%), sodium carbonate (Macron 100%), sodium chloride (Macron, 100%), and sodium phosphate monohydrate (Macron, 99.2%) were obtained from VWR. 3-Glycidoxypropyltrimethoxysilane ($\geq 98\%$) and 3-Amino-1-propanesulfonic acid (97%) were purchased from Sigma-Aldrich. All heating of reaction vessels was done in a Quincy Lab Model 10AF convection oven regulated by a Red Lion T48 PID controller accurate to within 0.1°C.

Chemical Structures of Target Control, and Probe DNA



Probe ssDNA: 5'-NH₂-GT CGG TAT ATC CCA T-3'

12-mer Target ssDNA: 3'-CC ATA TAG GGT A-5'-PEG₆-Cy3

10-mer Target ssDNA: 3'-ATA TAG GGT A-5'-PEG₆-Cy3

Control ssDNA: 3'-TAG ATG ATG A-5'-PEG₆-Cy3

Figure S-1. Chemical structures of fluorescently-labeled 10-mer and 12-mer (added in gray) target-ssDNA, left, and amine-terminated probe ssDNA, right. Below are the sequences of probe (blue), 12-mer target (green), 10-mer target (purple), and control (red) ssDNA.

Oligonucleotide Immobilization onto Glass Surfaces.

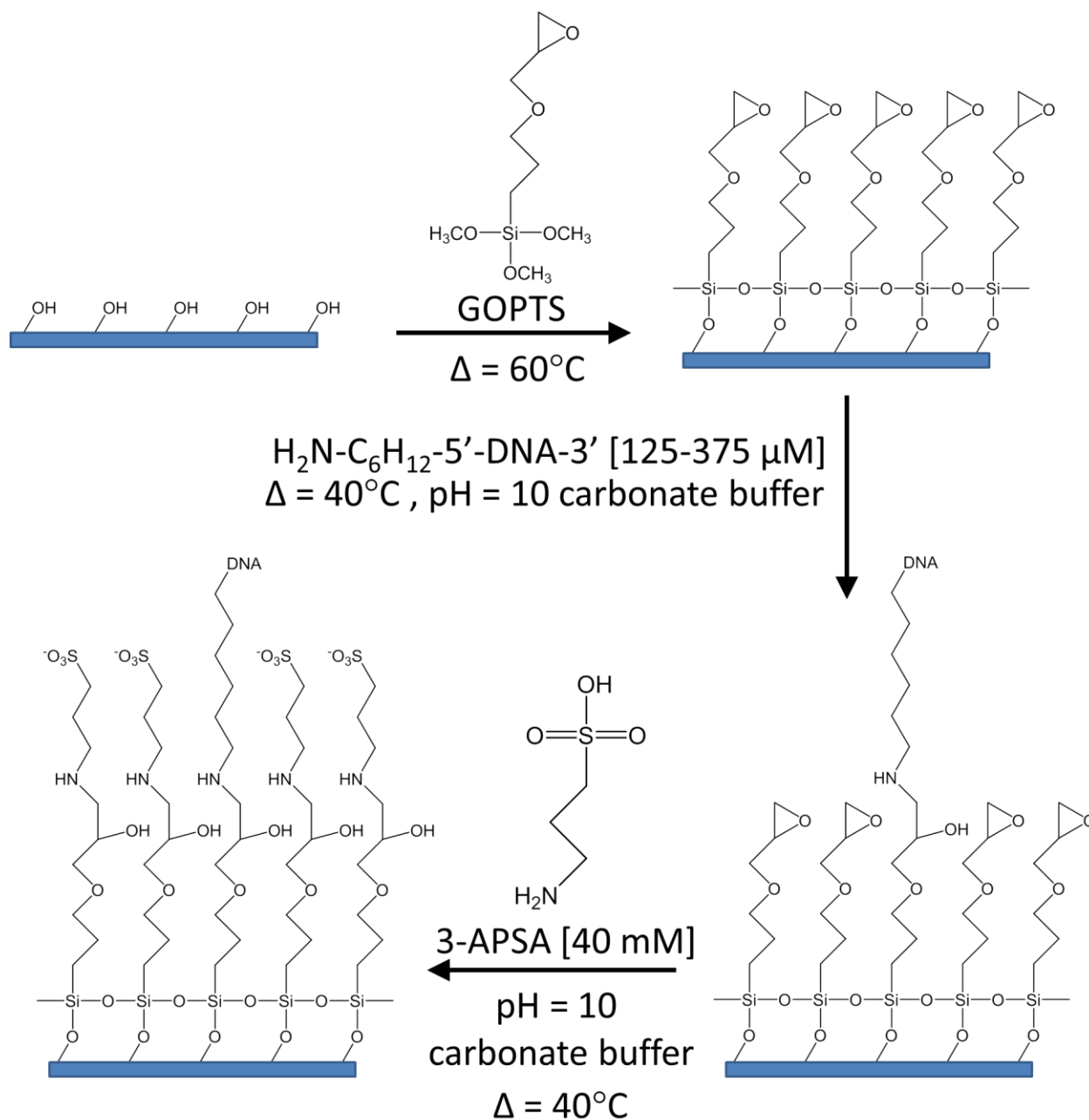


Figure S-2. Reaction scheme for probe immobilization and surface passivation on GOPTS-modified glass substrates. The amine-DNA concentration in the first step was varied from 125 to 375 μM .

Image Analysis for Detecting and Counting Single Molecules

Image analysis for counting bound molecules and measuring residence times and fluorescence intensities was performed using programs written in for Matlab 2012b (Mathworks). Images were prepared for analysis by converting pixel intensity values from arbitrary counts in analog-to-digital units (ADU), I_{ADU} , into photoelectron (PE) counts, I_{PE} , using a scaling factor methodology developed by Mortara et al.¹ Photoelectron counts exhibit Poisson-like error where the count variance equals twice their mean, $v_{\text{PE}} = 2\mu_{\text{PE}}$, where the electron multiplying amplifier on the EMCCD camera doubles the variance of the measured charge relative to the Poisson photoelectron limit.² The measured variance and mean in ADU^2 and ADU, respectively, for images of uniform white noise follow the expected linear relationship, as shown in Figure S-3. A plot of pixel ADU variance versus the ADU mean exhibits a slope, m , which can be used to convert I_{ADU} to I_{PE} , using the following relationship:

$$I_{\text{PE}} = \frac{2}{m} (I_{\text{ADU}}) \quad [\text{S1}]$$

Single molecule spots with signal-to-noise ratios of ~ 6 were detected using an intensity threshold that relies on the finite size of the diffraction-limited point spread function (PSF).³ Single-molecule spots were detected by locating $0.5 \times 0.5 \mu\text{m}$ (3×3 pixel) regions with three or more pixels brighter than an intensity threshold, I_{thold} , set at n_{std} -times the background standard deviation, σ_{bg} , above the mean background intensity, μ_{bg} : $I_{\text{thold}} = n_{\text{std}}\sigma_{\text{bg}} + \mu_{\text{bg}}$. The spatial resolution limit of the detection scheme was set by a $0.42 \mu\text{m}$ radius circle, defining the minimum separation distance between molecules. Within the minimum separation distance, the coordinates for each molecule were measured with sub-pixel precision by calculating the molecule's intensity center-of-mass.

Mean background intensities for each video were estimated by locating the peak value in a histogram of I_{PE} . An example I_{PE} histogram for 10 pM target ssDNA over a 250 μM probe-ssDNA surface is shown as the open circles in Figure S-4. We determine the standard deviation of the background intensity taking advantage of the Poisson-like error of the background intensity. Since $v_{\text{bg}} = 2\mu_{\text{bg}}$ (see above) the background noise standard deviation can be estimated from the mean background value: $\sigma_{\text{bg}} = (2\mu_{\text{bg}})^{1/2}$. By increasing n_{std} , I_{thold} increases and fewer spurious noise spots are detected as false positives. If the threshold is set too high, the intensity of actual molecule PSFs will not exceed I_{thold} and molecules will be missed, increasing the probability of false negative events.

As shown in Figure S-5, the distribution of target DNA intensities detected with $n_{\text{std}} = 3.0$, $I_{\text{thold}} = 20$ PE, (black curve) appears to have two well-separated distributions: one is centered at 60 PE, while the other is cut off by the threshold. The target DNA intensity distribution near the threshold is very similar in shape and magnitude to that of spurious molecules detected on the surface with blank buffer alone (red curve), leading us to conclude that these buffer contaminant molecules are the source of the low intensity distribution in the target DNA intensity histogram. When detecting single molecules in an image, n_{std} was set to 6.0 to exclude this population of spurious contaminant molecules in the buffer. Such a high n_{std} results in an infinitesimally small false positive probability due to background photon shot noise,³ while reducing the number of contaminant molecules detected in blank buffer from ~11 molecules per frame with a threshold of 3.0 standard deviations of the background, to ~1 molecule per frame at a threshold of 6.0 standard deviations.

False negative probabilities were determined from histograms of the “critical pixel” intensity, I_{crit} . The critical pixel is the third most intense pixel in the PSF, and determines whether the spot meets the intensity threshold. A histogram of I_{crit} for molecules detected in 10-pM target ssDNA for the 250 μM probe-ssDNA surface is plotted in Figure S-4, along with a Gaussian function fit. The lower edge of the I_{crit} histogram is cut off by I_{thold} , set at 30 PE; any spots less intense than the threshold will not be counted. The fraction of molecules above the intensity threshold can be calculated from the ratio of the integrated area above I_{thold} to the integral of the whole function. The fraction of molecules detected is 99 %, resulting in a false negative probability of only 1 %.

To calculate equilibrium surface populations for the 10-mer target, probe-target complexes were counted in typically 10 individual images captured at equilibrium. Videos were sampled in time intervals corresponding to twice the molecule unbinding time, ~50 s, to ensure sampled populations were uncorrelated and accurately represented counting uncertainties.

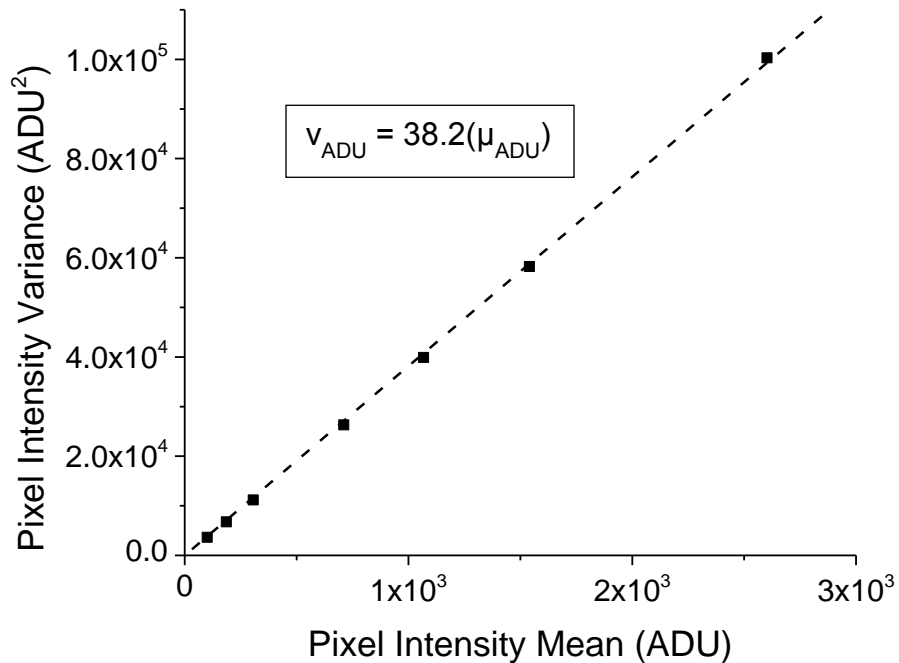


Figure S-3. ADU variance versus mean plot to determine photoelectron conversion factor, I_{ADU} is plotted as black squares, and the best fit line plotted as the dashed line, with equation shown.

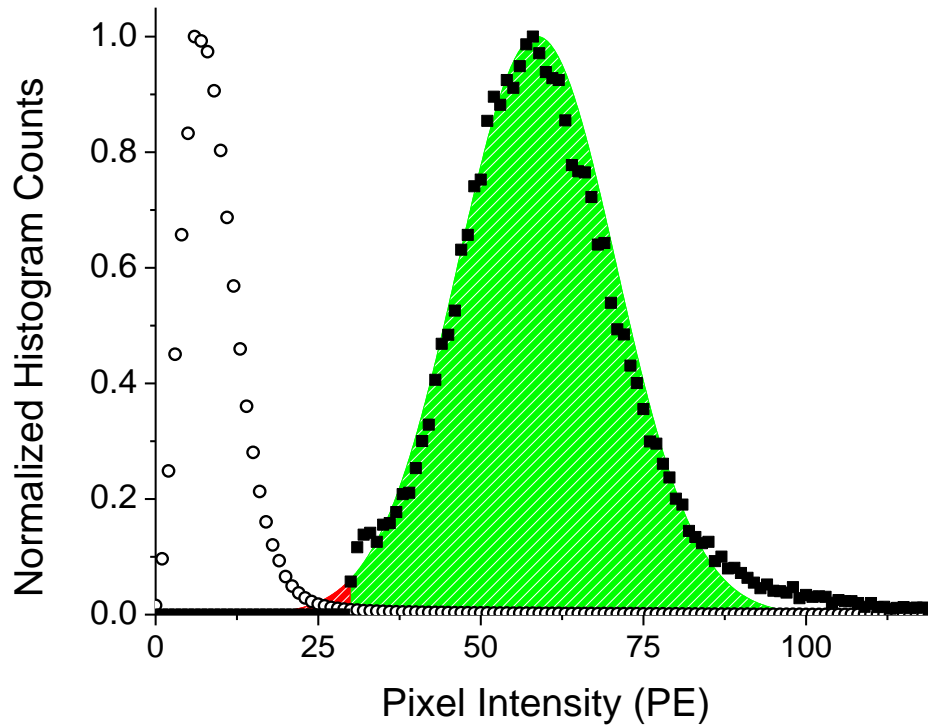


Figure S-4. I_{PE} histograms: comparison of blank background (open circles) and third most intense (critical) pixel intensity (black squares); an exponentially modified Gaussian function fit as shown with fraction below threshold colored red (1 %), and section above threshold colored green (99%).

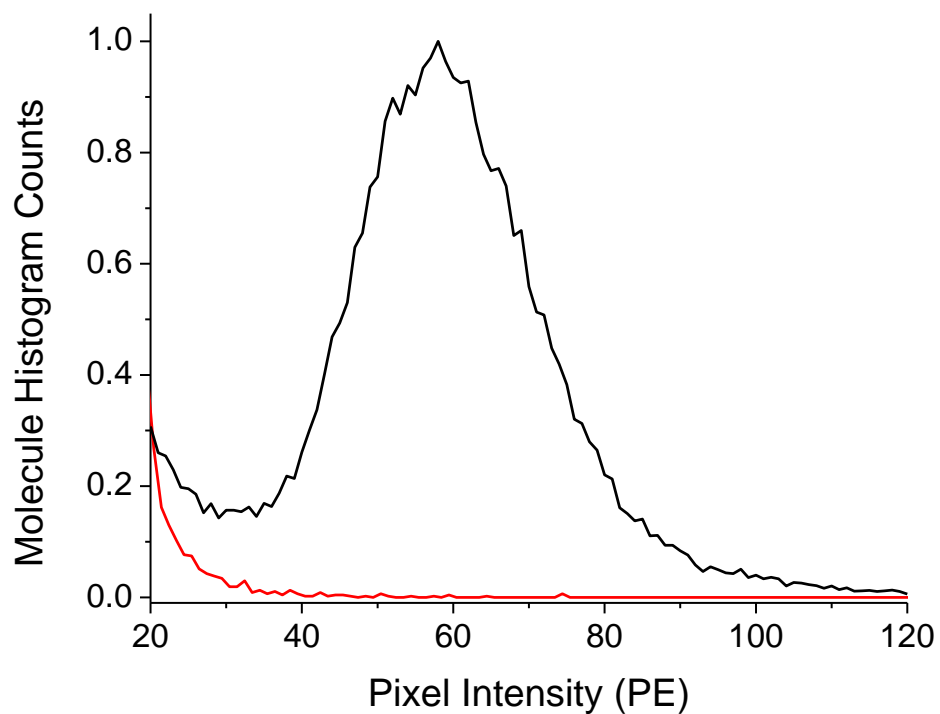


Figure S-5. I_{PE} histograms of targets and contaminants: target DNA molecule intensity, 50 pM, (black line) and contaminant molecule intensity, blank buffer (red line), show similar shape and magnitude at low I_{thold} .

Measuring Γ_{\max} with 12-mer target ssDNA

Another simple way to mitigate background fluorescence from solution is to simply increase the association constant of the binding interaction: at lower K_d , lower solution concentrations are needed to achieve the same hybridized dsDNA surface coverage. It is trivial to decrease the K_d of DNA hybridization pairs by simply increasing the number of complementary base pairs.⁴ Since the immobilized probe is a 15-mer, a 12-mer target strand with two additional base pairs can be introduced to the flow cell and used to interrogate the *same probe strands* in the *same region of the surface* used to measure a 10-mer isotherm. We can use a Γ_{\max} determined with a 12-mer target to interpret a single-molecule (low concentration) isotherm measured with a 10-mer probe, comparing the resulting values of K_d as a test of the consistency of the two approaches to determining Γ_{\max} .

Images of fluorescence from the interface are collected with an Andor iXon DU897 electron-multiplying charge-coupled device in a 256-by-256 pixel region, corresponding to a 40-by-40- μm area at the sample. Images were collected using 500-ms integrations in 2.0-s time-lapse intervals, at an electron-multiplying gain of 150x and a readout speed of 10MHz. Illumination intensity of 2.5 mW (3.75 W cm^{-2} during illumination, 0.95 W cm^{-2} averaged over 2-s intervals) was used to minimize photobleaching.

The measured calibration curve used to convert images from ADU to PE for images of uniform white noise with camera settings used for 10-mer and 12-mer target imaging are shown in Figure S-6. Single molecule spots in data sets with 12-mer and 10-mer target were detected with signal-to-noise ratios of ~ 3.2 using an intensity threshold, as described above.³ The spatial resolution limit of the detection scheme was set by a 0.42 μm radius circle, defining the minimum separation distance between molecules. A histogram of I_{crit} for molecules detected in 100 pM target ssDNA for the 12-hour probe-ssDNA surface is plotted in Figure S-7, along with an empirical exponentially modified Gaussian function fit.³ The lower edge of the I_{crit} histogram is cut off by I_{thold} , set at 89 PE; any molecules less intense than the threshold will not be counted. The fraction of molecules detected is 98.5%, resulting in a false negative probability of 1.5%.

To calculate equilibrium surface populations for the 10-mer target, probe-target complexes were counted in 15 individual images captured 10 min after sample injection. For the 12-mer target, probe-target complexes were counted in 5 individual frames captured 20 min after sample injection. Videos were sampled in time intervals corresponding to twice the molecule

unbinding time, ~ 50 s, to ensure sampled populations were uncorrelated and accurately represented counting uncertainties. The 12-mer dissociation time is very long (~ 10 min.), so it was difficult to maintain focus over the time needed to refresh the surface population. For this reason, the reported populations of 12-mer targets were taken from an average of several frames of videos collected within 10-20 s, providing a single measure of the instantaneous molecule population. Since counting molecules is a Poisson-like process, the reported 95% confidence limit for the 12-mer target population is reported as twice the square root of the average population. The relative standard deviation for typical molecule populations of ~ 100 is expected to be around 10%, which provides a significant contribution to the uncertainty of parameters determined from the accumulation isotherm (Γ_{\max} and K_a).

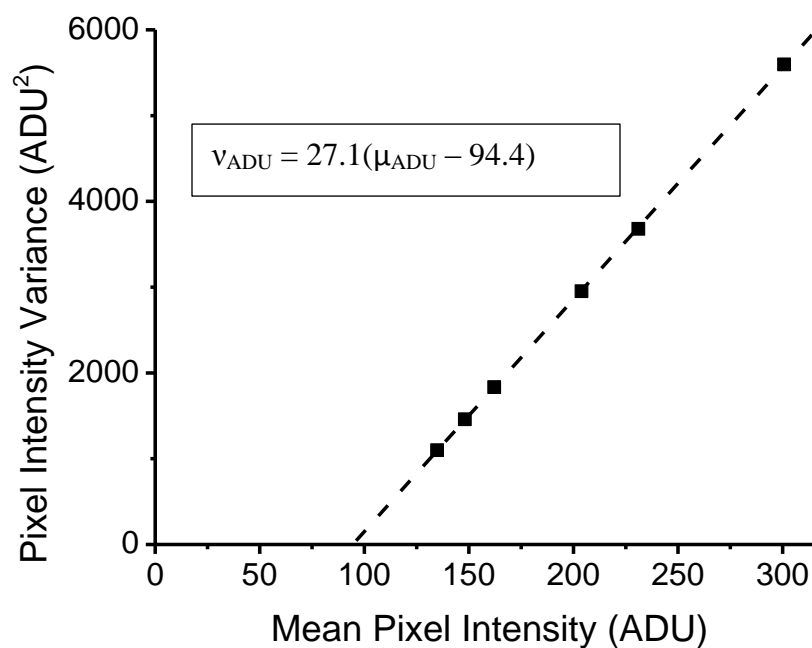


Figure S-6. ADU mean-variance plot to determine photoelectron conversion factor, I_{ADU} is plotted as black squares, and the best fit line plotted as the dashed line, with equation shown.

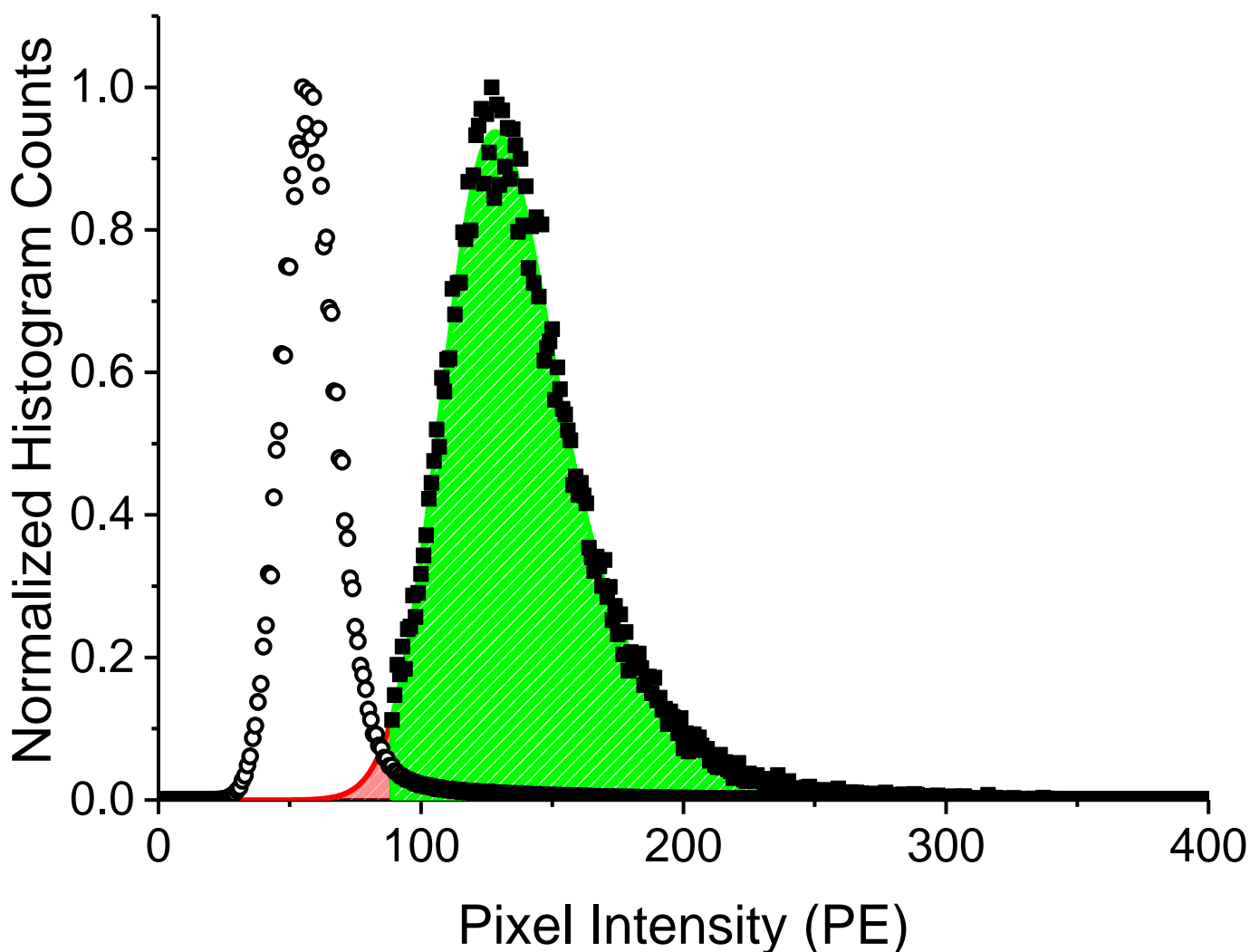


Figure S-7. I_{PE} histograms: comparison of blank background (open circles) and third most intense (critical) pixel intensity (black squares); an exponentially modified Gaussian function fit as shown with fraction below threshold colored red (5%), and section above threshold colored green (95%).

Single molecule isotherms of 10-mer and 12-mer target hybridization are shown in Figure S-8 for two different substrates with low and high surface density, which are designated “12-hour” and “24-hour” for the respective probe immobilization reaction times. The slope of the 12-hour, 12-mer target isotherm, $\Gamma_{\max} \times K_a$ is ~ 40 times greater than that of the 10-mer target isotherm, indicating that K_a is 40 times larger. At a $[DNA_{t12}] = K_d$ of 1.5 nM (see below), the

labeled target molecule population in the evanescent wave is less than 1% of the surface-bound population, making the background fluorescence from solution negligible. Fluorescence intensities (Figure S-9) were measured for concentrations ranging from 1 pM to 2.5 nM by integrating intensity from the same 40- μm square region used to count single molecules; intensities were then calibrated with single molecule populations and fit to a Langmuir isotherm (Equation 1) as discussed previously.

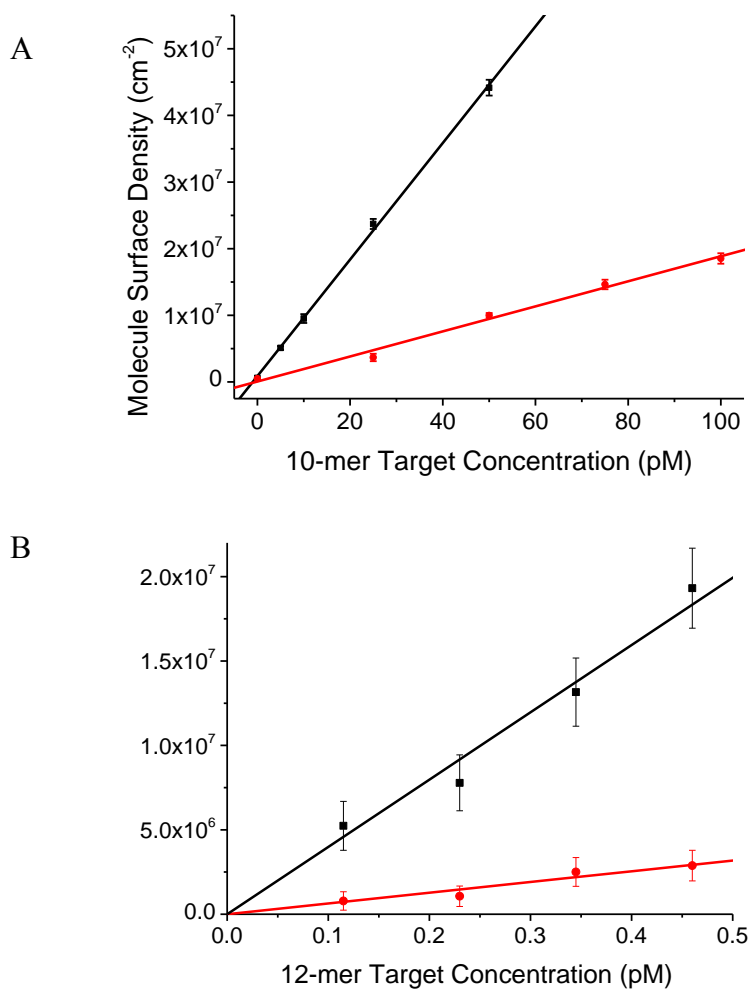


Figure S-8. Single molecule isotherm for A) 10-mer target ssDNA on 12-hour (red circles), and 24-hour (black squares) probe-immobilized surfaces, with best fit calibration lines from Eq. 2; and B) 12-mer target ssDNA isotherms.

The probe site density for 12-hour and 24-hour samples shows an expected increase, from $0.45 (\pm 0.07)$ to $2.5 (\pm 0.3) \times 10^{10} \text{ cm}^{-2}$, with immobilization reaction time increased from 12-hour and 24-hour. The K_a values, $1.42 (\pm 0.1)$ and $1.58 (\pm 0.07) \text{ nM}^{-1}$ respectively, for 12-mer target hybridization are within confidence intervals, further indicating that probe site density does not significantly influence the dissociation constant. With a measurement of Γ_{max} , K_a can be determined for 10-mer hybridization using Equation 2 and the single-molecule counting data in Figure S-8A. The K_a values for 10-mer target hybridization determined from the measured Γ_{max} and the low coverage linear isotherm are $41 (\pm 4)$ and $35 (\pm 2) \mu\text{M}^{-1}$ for 12-hour and 24-hour samples respectively. These K_a values show good agreement with the average K_a measured directly from full 10-mer target isotherms, $38.3 (\pm 0.3) \mu\text{M}^{-1}$, which supports the hybridization model. The agreement in K_a between high-coverage and low-coverage single-molecule isotherms indicates that Γ_{max} reports an equivalent probe density accessible to both 10-mer and 12-mer targets; and that the energetics of hybridization, represented by the slope of the isotherm, do not change with fractional coverage ranging from 0.1% (in the single molecule regime) to 67% (in the fluorescence intensity regime).

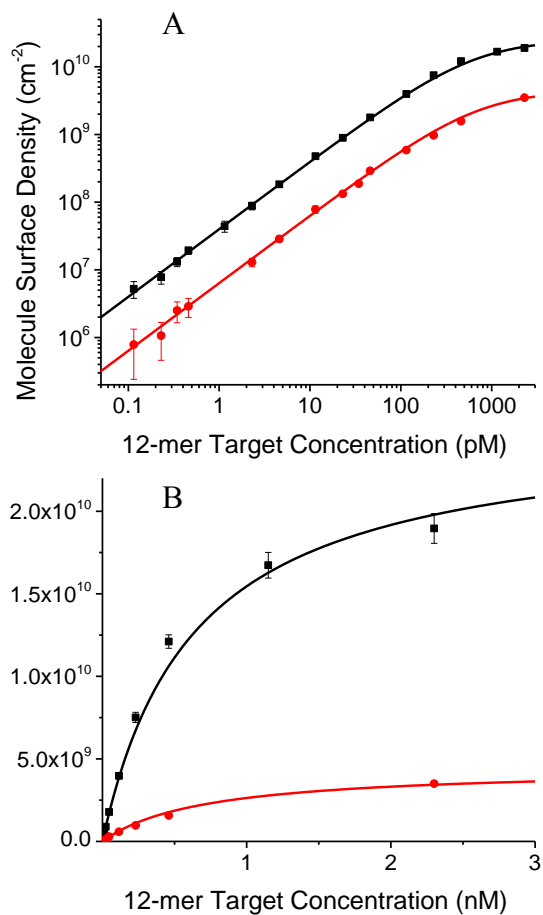


Figure S-9. Single molecule-calibrated bulk-fluorescence isotherm. A) single isotherm for 12 h (red circles) and 24 h surfaces (black squares) from Figure S-8B with calibrated average fluorescence intensity; B) calibrated fluorescence intensity isotherms with nonlinear best fit Langmuir isotherm from Equation 1.

Fluorescence Background Correction with Scrambled Cy3-ssDNA

When measuring the integrated fluorescence intensities of target ssDNA, the population of target molecules in free solution in the evanescent wave could contribute up to 5-20 % of the total fluorescence intensity. We measured this solution contribution to the total fluorescence signal using a scrambled Cy3-labeled 10-mer ssDNA, which does not adsorb to the surface, but contains an identical Cy3 label to the complementary target 10-mer. Interfacial fluorescence intensity was determined by integrating the intensity of fluorescence images over (43- x 43- μm) area to generate a background calibration, as shown for an example in Figure S-10. The background response is linear with scrambled 10-mer concentration, as expected for fluorescence from free-solution. A linear calibration line was fit to the background fluorescence data, and then subtracted from the fluorescence intensity measured for complementary target ssDNA, providing a measure of the fluorescence intensity from only the surface-bound duplex molecules as shown in Figure S-10.

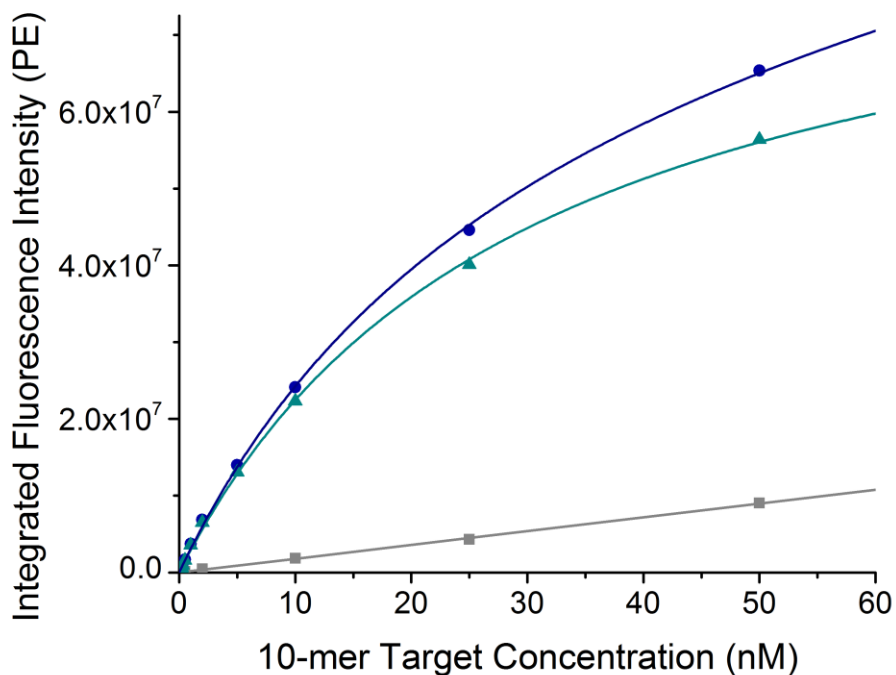


Figure S-10. Integrated interfacial fluorescence intensity for non-complementary scrambled ssDNA (gray squares) with linear calibration curve (gray line), raw fluorescence intensity for fully-complementary target ssDNA (dark blue circles) with Langmuir isotherm fit added to blank calibration curve (dark blue line), and blank-corrected target ssDNA intensity (light blue triangles) with Langmuir isotherm fit (light blue line).

Measuring Single-Molecule Residence Times

The residence time for each molecule on the surface was measured by tracking its intensity center of mass in sequential video frames. Starting at the beginning of a video, for every molecule coordinate the analysis program looks ahead in the subsequent video frame for a coordinate within a diffraction-limited detection radius of $0.33\ \mu\text{m}$ of the previous coordinate. If a match is found, the program continues stepping forward in time and repeats this process. When a molecule dissociates, no more matching coordinates will be found, and the program records the residence time.

Target ssDNA used in this study is labeled with one fluorophore and is subject to photobleaching and photoblinking. A molecule whose label is photobleached appears to unbind prematurely. Permanent photobleaching is mitigated by using low illumination intensities and time-lapse imaging. Photoblinking or transitions to short-lived dark states cause a molecule to flicker in intensity,^{5,6} and each brief light-dark transition may be mistaken for a binding-unbinding event. The impact of photoblinking was reduced by defining a “frame skip” time, τ_{fs} ,⁷ which allows the tracking program to look ahead several frames after a molecule has disappeared to see whether it returns. At sufficiently low densities of DNA, the probability of a new target ssDNA binding at the same coordinate as a molecule that departed seconds ago is negligible; therefore, it is more probable that the label on the original bound ssDNA entered a brief dark state. We found that τ_{fs} had little effect on single-molecule residence times, where τ_{fs} between 0 and 8 s increases apparent residence times by less than 10 %. The frame skip time was set to one video frame, or 2 s, in order to account only for the rare molecule missed due to the 1.5% false negative probability.

Residence times could be artificially extended if new target ssDNA binds near a previously detected molecule. The number of new molecules, N_{bind} , that bind near an existing molecule within the average residence time can be determined from the area of the site correlation tolerance, $A = 0.35\ \mu\text{m}^2$, the binding rate constant, $k_{\text{on}} = 1.6 \times 10^6\ \text{M}^{-1}\ \text{s}^{-1}$, the target ssDNA concentration $[\text{DNA}_t]$, the binding site density, $\Gamma_{\text{max}} = 45\ \text{to}\ 250\ \mu\text{m}^{-2}$, and $\tau = 24\ \text{s}$:

$$N_{\text{bind}} = \Gamma_{\text{max}} A k_{\text{on}} [\text{DNA}_t] \tau \quad [\text{S2}]$$

For every data set, residence times were only measured for target DNA concentrations predicted to keep N_{bind} less than around 0.05, corresponding to a $< 5\%$ chance of nearby binding.

Influence of Photobleaching on Measured Dissociation Rates

Dissociation times were measured for dsDNA complexes at illumination intensities between 2.7 and 8.2 W cm⁻² (with 0.2 ms light exposures every 2 s) to evaluate the influence of photobleaching on measured rates, as shown in Figure S-11. Dissociation rates were determined by fitting a double exponential decay function to cumulative histograms of single molecule residence times, as described above. There is a slight increasing trend in both the fast and slow component of k_{off} with illumination intensity, shown in Figure S-11 A and B, respectively, resulting in an increasing trend in the population-weighted dissociation rate, Figure S-11 C. The fast and slow decay components are both affected to similar degrees, indicating that photobleaching shifts the entire molecule lifetime distribution to shorter times, thereby reducing both the fast and slow decay components. This result suggests that both components of the lifetime distribution are due to DNA dissociation behavior rather than one of them being related to photophysical behavior of the label. The dissociation rate in the absence of photobleaching, k_{off}^0 can be estimated by extrapolating this linear trend to zero excitation power density. From a linear fit to the data in Figure S-11C, $k_{\text{off}}^0 = 0.041 (\pm 0.002) \text{ s}^{-1}$ (2 standard deviations of the mean), which is within uncertainty of the average dissociation rate of $k_{\text{off}} = 0.043 (\pm 0.002) \text{ s}^{-1}$ measured at 3.0 W cm⁻², indicating that photobleaching has little impact on the reported dissociation kinetics.

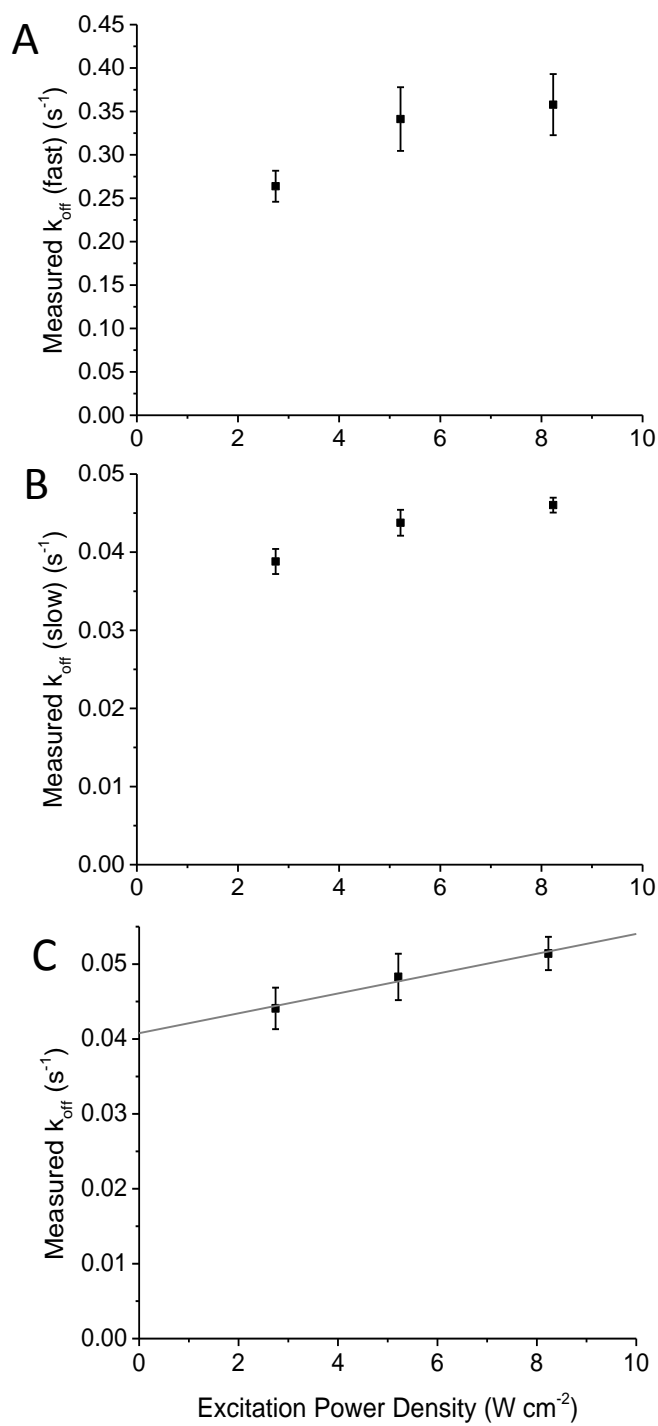


Figure S-11. Photobleaching analysis. Dissociation rates for 10-mer probe ssDNA, measured at multiple excitation power densities, A) fast dissociation component, B) slow dissociation component, C) population-weighted average dissociation rate.

High-Speed Imaging to Detect Adsorbed Target ssDNA

A separate TIRF microscope capable of high-speed imaging was used to test whether there is a significant population of mobile ssDNA molecules adsorbed to the sulfonate-passivated interface. This microscope has been used for molecule tracking⁸ and imaging fluorescence correlation spectroscopy.⁹ The high-speed microscope is equipped to illuminate a smaller region of the sample surface, increasing excitation power density to $\sim 160 \text{ W cm}^{-2}$, and utilizes a high-speed EMCCD camera, Andor iXon DU897 Ultra, capable of imaging at 100 Hz in a 256 by 256 pixel ($41 \times 41 \text{ }\mu\text{m}$ at 100x magnification) region. Videos were collected of 500 pM target ssDNA in 250 mM ionic strength buffer over a blank sulfonate-blocked surface.

Videos of 500 pM 10-mer target DNA are nearly featureless except for occasional immobile adsorbed molecules (surface population ~ 2 molecules/frame, see video ‘500 pM target sulfonate.avi’) and a diffuse fluorescence emission in the background. No moving molecules with a detectable signal-to-noise ratio could be tracked in the high-speed videos even at target DNA concentrations 5x higher than those used in single-molecule imaging experiments. We hypothesize that the background fluorescence is due to target ssDNA diffusing through the evanescent wave, since this background is not present in videos of buffer containing no target ssDNA. In order to verify this hypothesis, the fluorescence intensity of individual target molecules was compared to the fluorescence background of the target ssDNA solution. The average fluorescence emission intensity of 35 target molecules was determined by integrating the background-subtracted pixel intensity in an 8-by-8-pixel or 1.3-by-1.3- μm region that fully encompasses their point-spread-function. Average target solution background intensities were determined from the difference between the average pixel intensity from 500-pM target solution and the intensity from buffer alone, giving an average $I_0 = 560 (\pm 46)$ photoelectrons/molecule. The fluorescence intensity from images from the same area for 500-pM target ssDNA at the interface is $I = 37 (\pm 1)$ photoelectrons.

The expected fluorescence intensity from solution-phase molecules in the evanescent wave can be estimated as follows. The intensity, I , emitted by molecules in an evanescent wave is the integral over distance from the interface, z , of the product of the fluorescence intensity per molecule at the glass-solution interface I_0 , the detection area $A=(1.3\text{-}\mu\text{m})^2$, the target ssDNA concentration $[DNA_t] = 500 \text{ pM}$, Avogadro’s number N_A , and an exponential representing the

decay of evanescent wave excitation intensity from the surface, where the evanescent wave depth is $z_{ev} = 130$ nm.¹⁰

$$I = I_0[DNA_t]N_A A \int_0^\infty \exp(-z/z_{ev})dz = I_0[DNA_t]N_A A z_{ev} \quad [S3]$$

From Equation S3 and the measured I and I_0 , the target ssDNA (number per unit area) within the evanescent wave depth is $\Gamma_t = I/(I_0 A) = 3.9 (\pm 0.3) \times 10^6$ cm⁻²; this value is equivalent to the predicted target ssDNA in the evanescent wave, given by $\Gamma_t = [DNA_t]N_A z_{ev} = 3.9 \times 10^6$ cm⁻². The interfacial fluorescence from the target ssDNA solution at the blank sulfonate interface, therefore, can be entirely explained by solution-phase molecules in the evanescent wave. The uncertainty in the results sets an upper-bound (95% confidence)¹¹ on the adsorbed population (corrected for the higher excitation-rate at the surface) of $\Gamma_{t,ads} = 3.6 \times 10^5$ cm⁻² or ~9% of the population in the evanescent wave.

Fluorescence Hybridization Measurements in Free-Solution

The excitation spectrum (with emission monitored at 565 nm) and emission spectrum (excitation at 515 nm) of 2 nM Cy3-labeled target ssDNA is shown in Figure S-12. The emission spectra include 2 nM target ssDNA with no probe ssDNA (light orange), and 2 nM target ssDNA with 100 nM unlabeled probe DNA added (dark orange). Upon probe addition, emission intensity increased ~10%. Figure S-13 shows fluorescence time traces collected by continuously monitoring fluorescence emission intensity for a stirring solution of 2 nM Cy3-labeled target ssDNA. The red trace shows the increase in fluorescence emission of target DNA after addition of 100 nM probe ssDNA at the 30 s time mark. The black curve shows the response upon addition of 100 nM scrambled, non-complementary ssDNA; there is no time-dependent increase in target fluorescence emission, only a small drop in the baseline intensity.

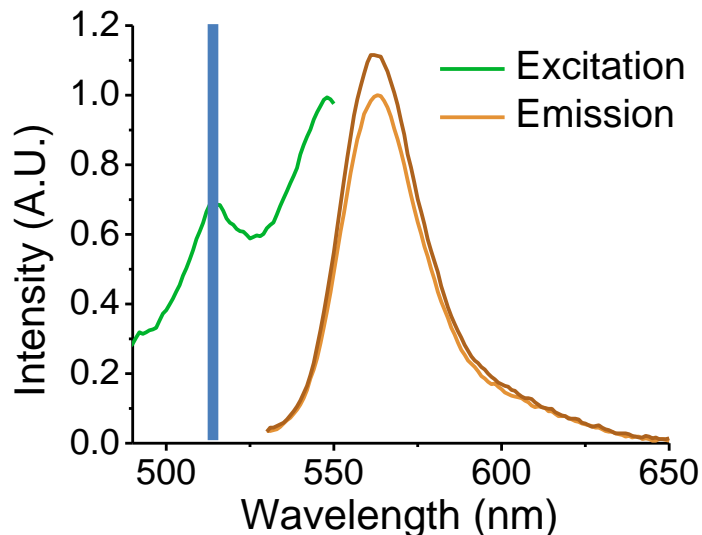


Figure S-12. 2 nM Cy3-labeled target 10-mer excitation spectrum (green) with excitation wavelength at 515 nm (blue line). Fluorescence emission spectra before (light orange), and after addition (dark orange) of 100 nM unlabeled probe 15-mer ssDNA.

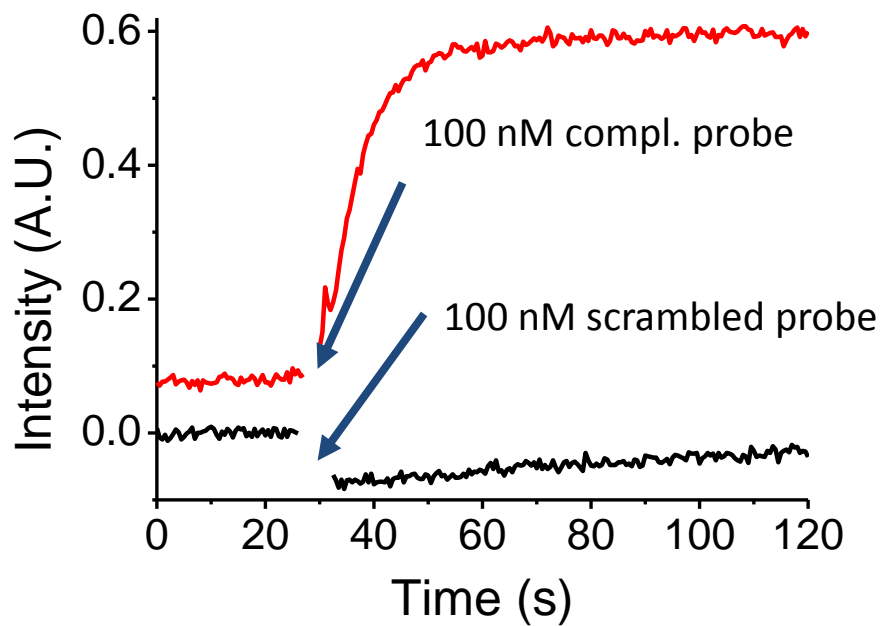
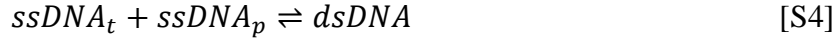


Figure S-13. Fluorescence intensity time traces of 2-nM Cy3-labeled target 10-mer ssDNA after addition of 100-nM complementary probe ssDNA (red line), and 100-nM scrambled ssDNA (black line) shows a small drop in the baseline, but no significant time-dependent change.

Derivation of Equilibrium Fluorescence Intensities for Free-Solution Hybridization.

Hybridization between target ssDNA and probe ssDNA is described by a reversible reaction:



The sum of the concentration of single stranded target DNA, $[ssDNA_t]$, and double-stranded target DNA, $[dsDNA]$, is equal to the total concentration of target DNA, $[DNA_t]$:

$$[DNA_t] = [ssDNA_t] + [dsDNA_t] \quad [S5]$$

At equilibrium, the fraction of hybridized DNA, is $\theta = [dsDNA_t]/[DNA_t]$, so that $[dsDNA_t] = \theta[DNA_t]$ and $[ssDNA_t] = (1 - \theta)[DNA_t]$. In the limit of low $[DNA_t]$ compared to the concentration of probe ssDNA, $[DNA_p]$, the hybridized fraction of target DNA can be expressed as a function of $[DNA_p]$ and the association constant, K_a :

$$\theta = \frac{K_a[DNA_p]}{1 + K_a[DNA_p]} \quad [S6]$$

As shown above, the two hybridization states of the Cy3-target DNA exhibit different fluorescence emission intensities on a per-molar basis, so that the total measured fluorescence intensity, I , is the sum of the fluorescence emission from single-stranded and double-stranded target DNA:

$$I = I_{ss}[ssDNA_t] + I_{ds}[dsDNA_t] \quad [S7]$$

where I_{ss} is the molar fluorescence emission coefficient for target ssDNA and I_{ds} is the fluorescence coefficient for duplex dsDNA. Substituting the expressions relating target concentrations to θ and $[DNA_t]$ into the expression for I :

$$I = (1 - \theta)I_{ss}[DNA_t] + \theta I_{ds}[DNA_t] \quad [S8]$$

Since I_{ss} , I_{ds} , and $[DNA_t]$ are constants for any given experiment, we combine them into new variables describing the pure single-stranded and double-stranded target fluorescence intensities: $I_{ss}^0 = I_{ss}[DNA_t]$ and $I_{ds}^0 = I_{ds}[DNA_t]$, so that

$$I = (1 - \theta)I_{ss}^0 + \theta I_{ds}^0 \quad [S9]$$

Substituting the expression relating θ to $[DNA_p]$ and the K_a into the equation above, we get a new expression for the total fluorescence intensity (Equation 5 in the main manuscript):

$$I = \frac{(I_{ds}^0 - I_{ss}^0)K_a[DNA_p]}{1 + K_a[DNA_p]} + I_{ss}^0 \quad [S10]$$

Description of Video Files

The file 'ac5b03832_si_002.avi' is a video of reversible 150 pM target ssDNA hybridization at a substrate with probe density of $4 \times 10^9 \text{ cm}^{-2}$. The video acquisition rate is 0.5 frames-per-second (fps), but it is played at 10x real time or 5 fps. Illumination and image acquisition settings are detailed in the main body of the paper. As can be seen in the video, single molecule spots reversibly adsorb to the surface with an average time of ~24 s.

The file 'ac5b03832_si_003.avi' is a video of 500 pM target ssDNA in contact with a blank substrate containing only sulfonate blocking groups. The video acquisition rate is 100 fps, but it is played at 1/10x real time, or 10 fps. Videos feature rare adsorption events, and a diffuse, rapidly moving background due to molecules diffusing through the evanescent wave.

References

- (1) Mortara, L.; Fowler, A. *Proc. SPIE* **1981**, *290*, 28-33.
- (2) Robbins, M.S.; Hadwen, B.J. *Electron Devices, IEEE Transactions on* **2003**, *50*, 1227-1232.
- (3) Peterson, E.M.; Harris, J.M. *Analytical Chemistry* **2010**, *82*, 189-196.
- (4) Jungmann, R.; Steinhauer, C.; Scheible, M.; Kuzyk, A.; Tinnefeld, P.; Simmel, F.C. *Nano Letters* **2010**, *10*, 4756-4761.
- (5) Moerner, W.E. *Science* **1997**, *277*, 1059.
- (6) Zondervan, R.; Kulzer, F.; Orlinskii, S.B.; Orrit, M. *The Journal of Physical Chemistry A* **2003**, *107*, 6770-6776.
- (7) Myers, G.A.; Gacek, D.A.; Peterson, E.M.; Fox, C.B.; Harris, J.M. *Journal of the American Chemical Society* **2012**, *134*, 19652-19660.
- (8) Cooper, J.T.; Peterson, E.M.; Harris, J.M. *Analytical Chemistry* **2013**, *85*, 9363-9370.
- (9) Cooper, J.T.; Harris, J.M. *Analytical Chemistry* **2014**, *86*, 7618-7626.
- (10) Hansen, W. *Journal of the Optical Society of America* **1968**, *58*, 380-390.
- (11) Currie, L.A. *Analytical Chemistry* **1968**, *40*, 586-593.